NANO LETTERS

Letter

pubs.acs.org/NanoLett

Bending Rigidity and Gaussian Bending Stiffness of Single-Layered Graphene

Yujie Wei,*[,†] Baoling Wang,[†] Jiangtao Wu,[†] Ronggui Yang,*[,‡] and Martin L. Dunn*[,‡]

[†]LNM, Institute of Mechanics, Chinese Academy of Sciences, Beijing 100190, P. R. China

[‡]Department of Mechanical Engineering, University of Colorado, Boulder, Colorado 80309, United States

ABSTRACT: Bending rigidity and Gaussian bending stiffness are the two key parameters that govern the rippling of suspended graphene—an unavoidable phenomenon of two-dimensional materials when subject to a thermal or mechanical field. A reliable determination about these two parameters is of significance for both the design and the manipulation of graphene morphology for engineering applications. By combining the density functional theory calculations of energies of fullerenes and single wall carbon nanotubes with the configurational energy of membranes determined by Helfrich Hamiltonian, we have designed a theoretical approach to accurately determine the bending rigidity and Gaussian bending stiffness of single-layered graphene. The bending rigidity and Gaussian bending stiffness of single-layered graphene are 1.44 eV (2.31×10^{-19} N m) and −1.52 eV (2.43×10^{-19} N m), respectively. The bending rigidity is close to the experimental result. Interestingly, the bending stiffness of graphene is close to that of lipid bilayers of cells about 1−2 eV, which might mechanically justify biological applications of graphene.

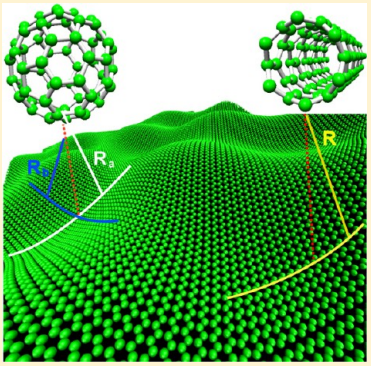

KEYWORDS: *Bending rigidity, Gaussian bending stiffness, graphene, Helfrich Hamiltonian, density functional theory*

The mechanical properties of graphene[1] are crucial to a variety of applications ranging from ultrafast electronics to nanocomposites and biological tissues.[2−4] The unique combination of a high modulus (∼1000 GPa) and tensile strength (∼100 GPa), which are 1−2 orders of magnitude higher than those of commonly used metals such as stainless steel, and extremely small out-of-plane stiffness make such one atomic layer thick graphene an ideal candidate for biological membranes and stretchable electronics applications.[4] The bending properties not only control the morphology of two-dimensional graphene under external field stimuli,[5−8] but also interplay with the electrical, magnetic, and thermal properties.[1,9−16] Compared to the modulus and the tensile strength of graphene, its bending rigidity and Gaussian bending stiffness are much less studied. In this work, we have designed a theoretical approach to accurately determine the bending rigidity and Gaussian bending stiffness of single-layer graphene, by combining the density functional theory calculations with the Helfrich Hamiltonian for membranes.

There are always concerns about the applicability of the existing continuum mechanics theories for characterizing the mechanical properties of graphene or carbon nanotubes (CNTs).[17] Instead of directly applying continuum mechanics theories to those low-dimensional carbon nanostructures, a combination of atomistic simulations with continuum theories is often used to deduce the mechanical properties of carbon nanostructures.[18−21] Although there exist several studies for the bending stiffness of graphene, either based on the combination of continuum theory and molecular dynamics simulations with empirical potentials[18−23] or by ab initio calculation,[24−29] there lack efficient and accurate methods to simultaneously determine both the bending rigidity (normal bending stiffness) and the Gaussian bending stiffness of free-standing graphene. In this work, we apply the density functional theory (DFT) calculations to obtain the energies of zero-dimensional fullerenes and one-dimensional single-walled carbon nanotubes (SWCNTs) of different radii. We then derive both the bending rigidity and the Gaussian bending stiffness of free-standing single layered graphene, which are work-conjugate to the square of mean curvature and the square of Gaussian curvature, respectively.

For a membrane with a three-dimensional topology (see illustration in Figure 1), we can write the configurational energy E described by the Helfrich Hamiltonian[30,31] as:

$$E = \int_S [\gamma + 2B_M(C_M - C_0/2)^2 + B_G C_G]dS \quad (1)$$

where γ is the energy for unitary flat surface, B_M is the bending rigidity, B_G is the Gaussian bending stiffness, $C_M = (k_1 + k_2)/2$ is the mean curvature whereas k_1 and k_2 are the two principal curvatures of a three-dimensional surface, $C_G = (k_1k_2)$ is the Gaussian curvature, and C_0 is spontaneous curvature, which disappears for symmetrical membranes. The integral in eq 1 extends over the whole surfaces. We can neglect C_0 without losing the accuracy in our following discussions due to the symmetry feature of fullerenes, SWCNTs, and graphene.

Received: August 26, 2012
Revised: November 14, 2012
Published: December 5, 2012

   dx.doi.org/10.1021/nl303168w | *Nano Lett.* 2013, 13, 26−30

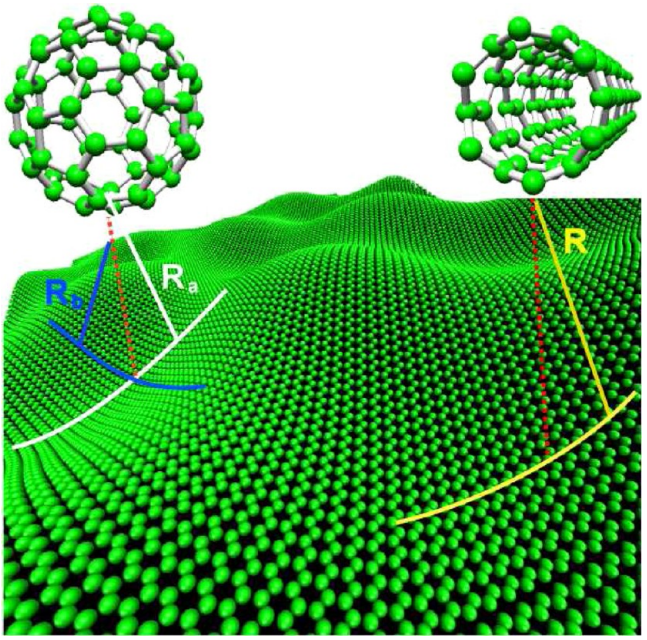

Figure 1. Illustration for the determination of the two elastic parameters controlling the corrugation of graphene. Given the geometrical nature of fullerenes and single wall carbon nanotubes, we need two curvature parameters ($k_1 = 1/R_a$ and $k_2 = 1/R_b$) to describe the bending characteristics of a fullerene but one ($k = 1/R$) for a CNT. This feature enables us to quantify the bending rigidity and Gaussian bending stiffness of graphene by adopting the Helfrich Hamiltonian.

By considering single layered graphene as a membrane, we assume that the surface energy γ remains to be constant during pure bending. It has also been recognized that there may exist in-plane strain in SWCNTs[19] and fullerenes. We have investigated the contribution of in-plane strain to the overall elastic energy in SWCNTs and fullerenes and found that the bending energy is at least one order-of-magnitude larger than that from in-plane deformation. This suggests the validity of eq 1 for samples considered here. By utilizing the fact that SWCNTs is a tube rolled up from a graphene,[32] we can decouple B_M from B_G by considering infinitely long constant-radius SWCNTs so that the term associated with the Gaussian curvature will disappear. By varying the radius of SWCNTs, we would then find that the energy per atom in SWCNT can be related to the energy per atom in graphene with the radii of SWCNTs by

$$E_{atom}^{CNT} = E_0 + S_0 B_M r^{-2}/2 \quad (2)$$

where r is the radius of SWCNTs, E_{atom}^{CNT} is the energy per atom in a SWCNT, E_0 is the energy of an atom in a flat graphene, and $S_0 = 3\sqrt{3}d^2/4 = 2.63$ Å^2 is the planar footprint of a carbon atom in graphene with d being the C−C bond length. By calculating the energy per atom in SWCNTs with different radii, it is straightforward to derive B_M, which is essentially the bending rigidity of graphene.

To determine the Gaussian bending stiffness B_G, we consider a series of spheroidal fullerenes with total atoms from 60 to 540, which have a corresponding radius variation from 1.86 Å to about 11 Å. Using eq 1, the energy per atom in fullerenes can be given as

$$E_{atom}^{F} = E_0 + S_0(2B_M + B_G)r^{-2} \quad (3)$$

where E_{atom}^{F} is the energy per atom in a fullerene, and r is the radius of a fullerene. In fullerene, the simplified average energy per atom shown in eq 3, which is obtained by dividing the total energy of a fullerene by its number of atoms, includes contributions from both bending deformation and pentagon rings. To obtain B_G for intact graphene, we need to correct E_{atom}^{F} by excluding the extra energy due to the presence of 12 pentagon rings in a fullerene. Since the 12 pentagon rings involve 60 atoms, which is the size of C_{60}, we will use the energy of C_{60} as a reference. For the total energy E_{total} of a fullerene with more than 60 atoms, we subtract E_{total} by the energy ΔE from the 60 atoms in 12 pentagons. The corrected energy per atom in the fullerene with more than 60 atoms is then obtained as

$$E_{atom}^{F} = \frac{E_{total} - \Delta E}{(N - 60)} \quad (4)$$

Now with B_M extracted using eq 2 from the calculation of SWCNTs, we could determine easily B_G by using eq 3 after obtaining E_{atom}^{F} for fullerenes of different radii. By using eq 4, we assume that the energy in a fullerene can be additively attributed to pentagons and hexagons, which is supported by the highly localized deformation by pentagons in fullerenes. Experiments show that the bond lengths of the fullerenes are about 0.145 ± 0.0015 nm for the bonds between pentagon and hexagon rings and 0.140 ± 0.0015 nm for the bond between the hexagon rings.[33] It suggests that the excessive energy by the

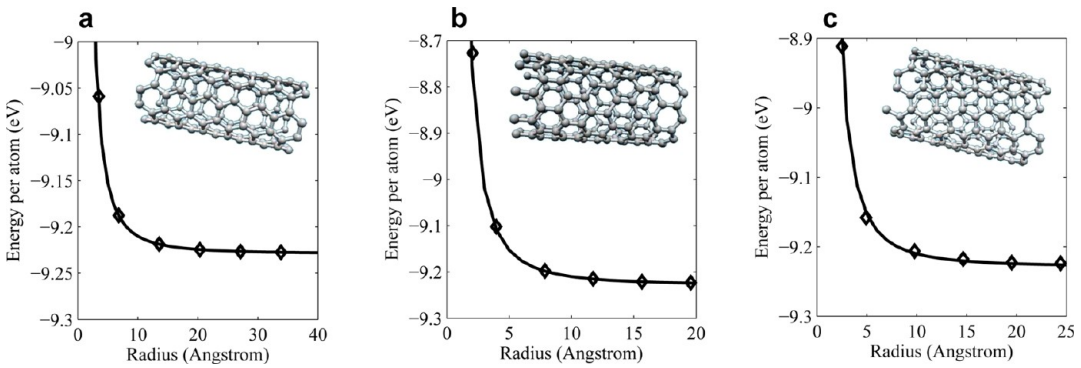

Figure 2. Energy per atom versus the radius in single-wall CNTs with different rolling up directions: DFT calculations (symbols) and continuum model (solid lines, with $B_M = 1.44$ eV). (a) Rolled up along the armchair indices. (b) Rolled up along the zigzag indices. (c) Rolled up along the chiral indices ($n = 5i$, $m = 2i$) for $i = 1$−6. The insets in each figure show the typical tube structures.

dx.doi.org/10.1021/nl303168w | *Nano Lett.* 2013, 13, 26−30

12 pentagons are highly localized and can be well-represented by the reference energy of C_{60}.

We use DFT calculations to obtain the energies per carbon atom in SWCNTs and fullerenes. The calculations were performed using the Vienna Ab Initio Simulation Package (VASP)[34,35] with the projector augmented wave (PAW) method and the Perdew–Burke–Ernzerhof (PBE) generalized gradient approximation (GGA) for the exchange and correlation terms. A plane-wave basis set with a kinetic energy cutoff of 400 eV and a Monkhorst-Pack k-point mesh are used. Atoms are relaxed using a conjugate gradient algorithm until the interatomic forces are less than 0.03 eV/Å.

For SWCNTs, the periodic boundary condition in the tube axis direction is applied. The vacuum space in nonperiodic directions (the radial direction) is set to be 1 nm to avoid interactions of SWCNTs or fullerenes with their periodic images. It is well-known that SWCNTs is commonly indexed by two integers (n,m), from which the radius r and the chiral angle χ can be deduced.[32] As a reference, the energy per carbon atom in an infinite free-standing graphene (approximated by applying periodic boundary conditions in the length direction) is also calculated. In the absence of deformation, the C–C bond length is calculated to be d = 0.1422 nm in the ideally flat graphene, which is in good agreement with the experimental value of 0.1421 nm.[32] The energy per atom in the ideally flat graphene is at E_0 = −9.229 eV.

Figure 2 shows the calculated energy per carbon atom in SWCNTs of different radii. Figure 2a shows the E_{atom}^{CNT} versus r curve for SWCNTs with the tubes rolled up along the armchair direction (see the inset). The theoretical fitting to eq 2 renders the bending rigidity B_M = 1.44 eV. This value is consistent with previous DFT calculations, as seen in Table 1. Figure 2b and c shows E_{atom}^{CNT} versus r for SWCNTs rolled up along the zigzag and along the chiral indices of (n = 5k, m = 2k where k = 1, ..., 6), respectively. By fitting the numerical calculation results to eq 2, we essentially obtained the same value of bending rigidity B_M as that for the SWCNT rolled up along the armchair direction, which indicates that the bending rigidity is almost the same for SWCNTs with different chiralities. This result is indeed consistent with previous reports using DFT calculations, which showed that graphene is nearly isotropic at small strains, with Young's modulus E = 1050 GPa and Poisson's ratio υ = 0.186.[24,25]

Table 1. Bending Rigidity and Gaussian Bending Stiffness of Single-Layered Carbon Structures[a]

authors [reference]	B_M (eV)	B_G (eV)	method
this study	1.44	−1.52	DFT
Sanchez-Portal et al.[26]	1.52	N/A	DFT
Kudin et al.[24]	1.4–1.46	N/A	DFT
Muñoz et al.[29]	1.48	N/A	DFTB
Koskinen and Kit[28]	1.61	−0.7	DFTB
Tersoff[22]	1.02	N/A	empirical potential
Tu and Ou-Yang[23]	1.17	N/A	empirical potential
Arroyo and Belytschko[27]	0.83	N/A	empirical potential
Lu et al.[19]	1.4	N/A	empirical potential
Nicklow et al.[39]	1.2	N/A	experiments

[a]Here DFTB is the abbreviation of density functional tight-binding model.

Following the logic presented before, we can now determine the Gaussian bending stiffness of graphene by performing DFT calculations for fullerenes, after the calculation of the bending rigidity of graphene through DFT calculations of SWCNTs. Fullerenes form a spheroid shape with 12 pentagons and a variable number of hexagons.[36−38] Table 2 gives the detailed information for fullerenes of different size after structure relaxation. Figure 3 gives the detailed geometries of several fullerenes including C_{60}, C_{80}, C_{180}, C_{320}, C_{500}, and C_{540}. For better viewing, atoms are colored based on their excessive energy in contrast to the energy of an atom in flat pristine graphene from corresponding molecular dynamics (MD) simulations. Here we have used MD package LAMMPS and adopted the AIREBO potential for carbon in our MD simulations. From the contour, we see that the excessive energy by the 12 pentagons are highly localized, which justifies the effectiveness when we apply eq 4. Clearly not all fullerenes are perfectly round. We have thus used the geometric mean of the three principal radii of a fullerene as the equivalent radius r. The principal radii are determined as follows. The a-axis is along the longest line connecting two pentagon poles in a fullerene. We could then determine the c-axis which is orthogonal to the a-axis but the shortest distance between the center and a point in the surface of the fullerene. The b-axis is found to be orthogonal to both a-axis and c-axis. The way to treat a fullerene as a sphere with the equivalent radius r essentially stems from the Gauss–Bonner theorem, which states that the integral of Gaussian curvature over the closed compact oriented surface M diffeomorphic to the sphere is equal to 2. The difference between the area of a fullerenes and the approximation by using an equivalent sphere is normally less than 1% for fullerene with more than 100 atoms.

Table 2. Properties for Fullerenes of Different Radii Obtained by DFT Calculations[a]

atoms (N)	K-point mesh	E_{total} (eV)	a-axis (Å)	b-axis (Å)	c-axis (Å)
60	2 × 2 × 2	−531.33	3.335	3.419	3.475
70	2 × 2 × 2	−622.58	3.465	3.542	3.973
76	2 × 2 × 2	−676.39	3.357	3.831	4.381
78	2 × 2 × 2	−693.86	3.576	3.679	4.298
80	2 × 2 × 2	−711.77	3.864	3.929	4.056
84	2 × 2 × 2	−748.46	3.277	4.250	4.791
100	2 × 2 × 2	−894.22	3.881	4.052	5.635
180	2 × 2 × 2	−1629.66	5.999	6.085	6.194
240	2 × 2 × 2	−2181.51	6.958	6.941	7.241
320	1 × 1 × 1	−2913.64	7.928	8.165	8.521
500	1 × 1 × 1	−4569.75	9.902	10.247	10.853
540	1 × 1 × 1	−4940.30	10.505	11.364	11.894

[a]The energy per atom converges gradually to the value E_0 of ideally flat graphene.

As discussed earlier for eq 4, we need to correct the energy per carbon atom in fullerenes before eq 3 can be successfully applied. Recall that C_{60} is the roundest one of all fullerenes, and each atom in a pentagon in C_{60} is shared by two hexagons, which is the case for all fullerenes with atomic number greater than 60. Therefore, we use the energy per atom in C_{60} as the reference value for atoms in pentagons in fullerenes. As seen in Table 2, ΔE = −531.33 eV is then used in eq 4 for the calculation of energy E_{atom}^{F} per atom in all fullerenes with more than 60 atoms. Figure 4a shows the energy per atom as a function of the equivalent radii of fullerenes with more than 60 atoms from DFT calculations. With B_M = 1.44 eV from the fitting of Figure 2, the DFT calculation results can be well-

dx.doi.org/10.1021/nl303168w | Nano Lett. 2013, 13, 26−30

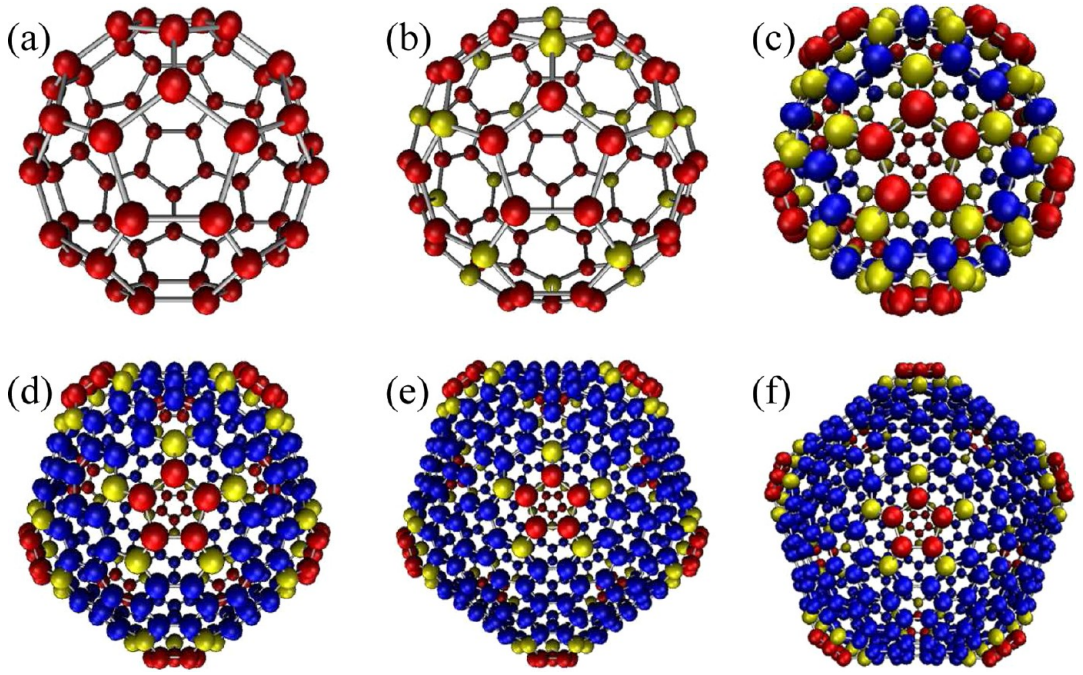

Figure 3. Energy contour from molecular dynamics simulations for fullerenes of different sizes. Atoms are colored based on the excessive energy in contrast to their reference energy state in flat graphene, with red, yellow, and blue, in turn, representing excessive energies about 0.60, 0.07, and 0.01 eV. (a) C_{60}, (b) C_{80}, (c) C_{180}, (d) C_{320}, (e) C_{500}, and (f) C_{540}. Note that each atom in a pentagon is shared by two other hexagons in fullerenes with an atom number greater than 60.

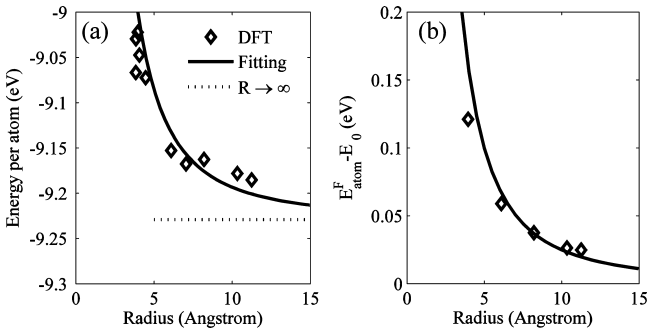

Figure 4. Energy per atom in fullerenes with different radii. (a) The results from DFT calculations (symbols), the fitted solid curve by the continuum model given in eq 3, and the energy per atom for ideally flat graphene (dashed line) are shown. The DFT calculations can be well-captured by eq 3 by taking $B_G = -1.52$ eV. (b) The results from MD calculations (symbols) can be well-captured by eq 3 by using the same bending stiffness and Gaussian bending rigidity from DFT calculations.

captured with $B_G = -1.52$ eV by fitting the results with eq 3. As a comparison we list in Table 1 our simulation results and those from the literature. The results from our MD calculations are shown in Figure 4b. Since E^F_{atom} in a fullerene is accessible from MD simulations, we do not need to use eq 4 here. Now the energy per atom in a fullerene is an average over all atoms except the 60 atoms associated with all pentagons in the fullerene. $E^F_{atom} - E_0$ from MD simulations can be well-described by eq 3 with the same bending stiffness and Gaussian bending rigidity from DFT calculations.

In contrast, the continuum mechanics-based Kirchhoff–Love theory for thin plates predicts $B_M = 22.3$ eV (with $B_M = EH^3/12(1 - \upsilon^2)$, $E = 1050$ GPa, and $\upsilon = 0.186$[26−28]) with $H = 0.34$ nm used as the thickness of single layered graphene, which is one order-of-magnitude higher than the result reported here. This discrepancy indicates the breakdown of the applicability of continuum theory to predict bending properties in graphene. We note that there are discussions that H may not be 0.34 nm for single layered graphene[19,27,28] and a smaller effective thickness might reconcile the difference for B_M between the prediction by continuum mechanics theory and that from DFT calculation. The bending stiffness of single layered graphene is very close to those numbers of the lipid bilayers in cells,[31] which is about 1−2 eV. The parameters given here could be hence valuable for investigations about the interaction between the graphene and the cell member.[40]

In summary, by combining density functional theory calculations of carbon energies in the zero-dimensional fullerenes and one-dimensional single-walled carbon nanotubes, with the Helfrich Hamiltonian for the configurational energy of membranes, we determined the bending rigidity and Gaussian bending stiffness of single-layered graphene to be 1.44 eV (2.31×10^{-19} N m) and −1.52 eV (2.43×10^{-19} N m), respectively. These two elastic parameters of graphene are crucial for structure and morphology manipulation in the proposed biological and stretchable electronic applications.

AUTHOR INFORMATION

Corresponding Author

*E-mail: (Y.W.) yujie_wei@lnm.imech.ac.cn; (R.Y.) ronggui.yang@colorado.edu; and (M.D.) martin.dunn@colorado.edu.

Notes

The authors declare no competing financial interest.

ACKNOWLEDGMENTS

The authors acknowledge support from the Chinese Academy of Sciences and MOST 973 of China (No. 2012CB937500) and National Natural Science Foundation of China (NSFC)

(11021262) (Y.J.W.) and AFOSR (Grant No. FA9550-11-1-0109) (R.G.Y.).

REFERENCES

(1) Novoselov, K. S.; Geim, A. K.; Morozov, S. V.; Jiang, D.; Zhang, Y.; Dubonos, S. V.; Grigorieva, I. V.; Firsov, A. A. *Science* **2004**, *306*, 666. Geim, A. K. *Science* **2009**, *324*, 1530.
(2) Iijima, S. *Nature* **1991**, *354*, 56.
(3) Wong, E. W.; Sheehan, P. E.; Lieber, C. M. *Science* **1997**, *277*, 1971.
(4) Rogers, J. A.; Lagally, M. G.; Nuzzo, R. G. *Nature* **2011**, *477*, 45.
(5) Yakobson, B. I.; Brabec, C. J.; Bernholc, J. *Phys. Rev. Lett.* **1996**, *76*, 2511.
(6) Liu, Y.; Yakobson, B. I. *Nano Lett.* **2010**, *10*, 2178.
(7) Yakobson, B. I.; Ding, F. *ACS Nano* **2011**, *5*, 1569.
(8) Fasolino, A.; Los, J. H.; Katsnelson, M. I. *Nat. Mater.* **2007**, *6*, 858.
(9) San-Jose, P.; Gonzalez, J.; Guinea, F. *Phys. Rev. Lett.* **2011**, *106*, 045502.
(10) Schebarchov, D.; Hendy, S. C.; Ertekin, E.; Grossman, J. C. *Phys. Rev. Lett.* **2011**, *107*, 185503.
(11) Guinea, F.; Geim, A. K.; Katsnelson, M. I.; Novoselov., K. S. *Phys. Rev. B* **2010**, *81*, 035408.
(12) Liu, P.; Zhang, Y. W. *Appl. Phys. Lett.* **2009**, *94*, 231912.
(13) Schniepp, H. C.; Kudin, K. N.; Li, J.-L.; Prud'homme, R. K.; Car, R.; Saville, D. A.; Aksay, I. A. *ACS Nano* **2008**, *2*, 2577.
(14) Cadelano, E.; Palla, P. L.; Giordano, S.; Colombo, L. *Phys. Rev. B* **2010**, *82*, 235414.
(15) Zhang, Z.; Liu, B.; Hwang, K. C.; Gao, H. *Appl. Phys. Lett.* **2011**, *98*, 121909.
(16) Li, X.; Maute, K.; Dunn, M. L.; Yang, R. G. *Phys. Rev. B* **2010**, *81*, 245318.
(17) Wei, Y.; Wu, J.; Yin, H.; Shi, X.; Yang, R. G.; Dresselhaus, M. S. *Nat. Mater.* **2012**, *11*, 759.
(18) Zhang, D. B.; Akatyeva, E.; Dumitrică, T. *Phys. Rev. Lett.* **2011**, *106*, 255503.
(19) Lu, Q.; Arroyo, M.; Huang, R. *J. Phys. D: Appl. Phys.* **2009**, *42*, 102002.
(20) Cadelano, E.; Palla, P. L.; Giordano, S.; Colombo, L. *Phys. Rev. Lett.* **2009**, *102*, 235502.
(21) Peng, J.; Wu, J.; Huang, K. C.; Song, J.; Huang, Y. J. *Mech. Phys. Solids* **2008**, *56*, 2213.
(22) Tersoff, J. *Phys. Rev. B* **1992**, *46*, 15546.
(23) Tu, Z. C.; Ou-Yang, Z. C. *Phys. Rev. B* **2002**, *65*, 233407.
(24) Kudin, K. N.; Scuseria, G. E.; Yakobson, B. I. *Phys. Rev. B* **2001**, *64*, 235406.
(25) Liu, F.; Ming, P.; Li, J. *Phys. Rev. B* **2007**, *76*, 064120.
(26) Sanchez-Portal, D.; Artacho, E.; Soler, J. M.; Rubio, A.; Ordejon, P. *Phys. Rev. B* **1999**, *59*, 12678.
(27) Arroyo, M.; Belytschko, T. *Phys. Rev. B* **2004**, *69*, 115415.
(28) Koskinen, P.; Kit, O. O. *Phys. Rev. B* **2010**, *82*, 235420.
(29) Muñoz, E.; Singh, A. K.; Ribas, M. A.; Penev, E. S.; Yakobson, B. I. *Diamond Relat. Mater.* **2010**, *19*, 368.
(30) Helfrich, W. *Z. Naturforsch. C* **1973**, *28*, 693.
(31) Lipowsky, R. *Nature* **1991**, *349*, 475.
(32) Saito, R.; Fujita, M.; Dresselhaus, G.; Dresselhaus, M. S. *Physical Properties of Carbon Nanotubes*; Imperial College London: London, 1998.
(33) Jonhson, R. D.; Bethune, D. S.; Yannoni, C. S. *Acc. Chem. Rec.* **1992**, *25*, 169.
(34) Kresse, G.; Furthmüller, J. *Phys. Rev. B* **1996**, *54*, 11169.
(35) Kresse, G.; Furthmüller, J. *Comput. Mater. Sci.* **1996**, *6*, 15.
(36) Krato, H. W.; McKay, K. *Nature* **1988**, *331*, 328.
(37) Smalley, R. E. *Acc. Chem. Res.* **1992**, *25*, 98.
(38) Diederich, F.; Whetten, R. L. *Acc. Chem. Res.* **1992**, *25*, 119.
(39) Nicklow, R.; Wakabayashi, N.; Smith, H. G. *Phys. Rev. B* **1972**, *5*, 4951.
(40) Frost, R.; Jönsson, G. E.; Chakarov, D.; Svedhem, S.; Kasemo, B. *Nano Lett.* **2012**, *12*, 3356.